appreciate the importance of oligosaccharides and glycoconjugates in nature.

References and Notes

1. R. A. Dwek, *Chem. Rev.* **96**, 683 (1996).
2. S. Hakomori, *Adv. Cancer Res.* **52**, 257 (1989).
3. G. J. Boons, Ed., *Carbohydrate Chemistry* (Blackie, London, 1998).
4. J. M. J. Frechet, C. Schuerch, *J. Am. Chem. Soc.* **93**, 492 (1971).
5. S. J. Danishefsky *et al.*, *Science* **260**, 1307 (1993).
6. P. H. Seeberger, W.-C. Haase, *Chem. Rev.* **100**, 4349 (2000).
7. R. Liang *et al.*, *Science* **274**, 1520 (1996).
8. M. H. Caruthers, *Science* **230**, 281 (1985).
9. E. Atherton, R. C. Sheppard, *Solid-Phase Peptide Synthesis: A Practical Approach* (Oxford Univ. Press, Oxford, UK, 1989).
10. Y. Ito, S. Manabe, *Curr. Opin. Chem. Biol.* **2**, 701 (1998).
11. Applied Biosystems Inc. Model 433A peptide synthesizer.
12. The machine was equipped with seven reagent bottles, four for washing and three for glycosylation and deprotection reagents. Small cartridges containing the donor species were loaded into the synthesizer manually before the synthesis. A cycle was programmed to operate all steps without any operator intervention. The machine controlled the delivery of all reagents and donor species to the reaction vessel and the mixing of the contents of the vessel.
13. B. Merrifield, *J. Am. Chem. Soc.* **85**, 2149 (1963).
14. M. A. J. Ferfuson, A. F. Williams, *Annu. Rev. Biochem.* **57**, 285 (1988).
15. R. Kornfeld, S. Kornfeld, *Annu. Rev. Biochem.* **54**, 631 (1985).
16. S. P. Douglas, D. M. Whitfield, J. J. Krepinsky, *J. Am. Chem. Soc.* **117**, 2116 (1995).
17. J. Rademann, R. R. Schmidt, *J. Org. Chem.* **62**, 3989 (1997), and references therein.
18. R. B. Andrade *et al.*, *Org. Lett.* **1**, 1811 (1999).
19. B. Yan, *Acc. Chem. Res.* **31**, 621 (1998).
20. For on-resin TOCSY analysis of **6**, see supporting data available on *Science* Online (*32*).
21. P. H. Seeberger *et al.*, *Angew. Chem. Int. Ed. Engl.* **36**, 491 (1997).
22. A. Darvill *et al.*, *Glycobiology* **2**, 181 (1992).
23. P. Fugedi *et al.*, *Carbohydr. Res.* **164**, 297 (1987).
24. K. C. Nicolaou *et al.*, *J. Am. Chem. Soc.* **119**, 449 (1997), and references therein.
25. O. J. Plante *et al.*, *Org. Lett.* **1**, 211 (1999).
26. D. Kahne *et al.*, *J. Am. Chem. Soc.* **111**, 6811 (1989).
27. N. M. Spijker, P. Westerduin, C. A. A. van Boeckel, *Tetrahedron* **48**, 6297 (1992).
28. H. Lonn, *Carbohydr. Res.* **139**, 105 (1985).
29. For a detailed description of the coupling cycle used, see the table in the supplemental information (*32*).
30. D. Bundle, S. Josephson, *Can. J. Chem.* **57**, 662 (1979).
31. P. P. Deshpande, S. J. Danishefsky, *Nature* **387**, 164 (1997).
32. Supplementary material is available at www.sciencemag.org/cgi/content/full/1057324/DC1.
33. Financial support from the American Chemical Society (ACS) Division of Organic Chemistry (Pfizer Graduate Fellowship for O.J.P.), the NIH Biotechnology Training Grant (fellowship for O.J.P.), and Merck (fellowship for E.R.P.) and partial funding from the ACS Petroleum Research Fund (ACS-PRF 34649-G1) and the Mizutani Foundation for Glycoscience are gratefully acknowledged. Funding for the MIT-DCIF Inova 501 was provided by NSF (award CHE-9808061) and the NMR facility at the Francis Bitter Magnet Laboratory was provided by the NIH (Grant RR-00995). We thank S. J. Lippard and J. Stubbe for their thoughtful discussion of this manuscript, S. S. Pochapsky for recording the HR-MAS NMR, and D. M. Ratner for assistance in modifying peptide synthesizers.

9 November 2000; accepted 23 January 2001
Published online 1 February 2001;
10.1126/science.1057324
Include this information when citing this paper.

Redox State of Mars' Upper Mantle and Crust from Eu Anomalies in Shergottite Pyroxenes

M. Wadhwa

The oxidation state of basaltic martian meteorites is determined from the partitioning of europium (Eu) in their pyroxenes. The estimated redox conditions for these samples correlate with their initial neodymium and strontium isotopic compositions. This is interpreted to imply varying degrees of interaction between the basaltic parent melts, derived from a source in the martian mantle, and a crustal component. Thus, the mantle source of these martian basalts may have a redox state close to that of the iron-wüstite buffer, whereas the martian crust may be more oxidized (with a redox state higher than or equal to that of the quartz-fayalite-magnetite buffer). A difference in redox state of more than 3 log units between mantle and crustal reservoirs on Mars could result from oxidation of the crust by a process such as aqueous alteration, together with a subsequent lack of recycling of this oxidized crust through the reduced upper mantle.

Determination of the redox state of Mars' mantle and crust would help to estimate elemental distributions between these silicate reservoirs and the core, thereby leading to a better understanding of the accretion and differentiation history of the planet. The red color of the martian surface is attributed to the presence of ferric minerals in the weathered, highly oxidized regolith (*1*). The silicate interior (that is, the mantle and crust) may be less oxidized than the regolith, but there are no direct estimates of its redox state. Indirect estimates of the oxidation state of the martian interior are mostly based on model compositions (specifically, FeO content) of the bulk silicate portion of Mars (BSM). Some of these compositions are derived from cosmochemical models with adjustable parameters fit to density distribution estimates from geophysical data (*2–6*). Others are from the bulk compositions of martian meteorites (*7–9*), which are currently the only samples of the crust of Mars available for study (*10*). A general feature of these models has been the prediction of FeO enrichment in the BSM relative to Earth's mantle, attributed to relatively oxidizing conditions on Mars.

Attempts to obtain estimates of redox conditions on Mars have also been made from the compositions of Fe-bearing minerals in the shergottites, a class of martian meteorites composed of basaltic and lherzolitic rocks, parent magmas of which are thought to represent fractionated partial melts of the martian mantle (*10*). Most of these studies rely on the compositions of coexisting Fe-Ti oxides (*11–14*) and indicate a range of oxidation conditions. However, because these oxides are among the very last phases to crystallize and are susceptible to subsolidus reequilibration, they may not record primary magmatic redox conditions. One investigation based on stoichiometric calculations of Fe^{3+}/Fe^{2+} in shergottite pyroxenes suggested that their source region in the martian mantle may be substantially reduced (*15*). However, a subsequent study (*16*) pointed out large uncertainties in the approach taken by (*15*). Therefore, the issue of the redox state of Mars' silicate interior has so far remained contentious.

Here, magmatic oxidation conditions for the basaltic shergottites were determined from the partitioning of Eu in the earliest crystallizing minerals. Eu is the only rare earth element (REE) than can exist in the divalent and trivalent states under magmatic conditions (other REEs are trivalent). The Eu mineral/melt distribution coefficient (D_{Eu}) for a particular mineral is dependent on the Eu^{3+}/Eu^{2+} ratio in the magma, which in turn is predominantly a function of the prevailing redox condition during crystallization (*17*). Partitioning experiments for synthetic high-Ca pyroxene (augite) and plagioclase with compositions similar to those in the angrites (a class of basaltic meteorites) have established the relation between D_{Eu}/D_{Gd} for these minerals (used as a proxy for the Eu^{3+}/Eu^{2+} ratio in the melt) and oxygen fugacity (f_{O_2}) (*18*). Although analogous experiments (that is, over a wide range of f_{O_2} conditions) have not been performed for the basaltic shergottites, the relation between D_{Eu}/D_{Gd} and f_{O_2} for shergottite minerals may be similar to that for angrite minerals because $(D_{Eu}/D_{Gd})_{augite}$ values from a set of experiments on a shergottite analog composition (*19, 20*) fall on the same curve as that defined by the data from

---

Department of Geology, The Field Museum, 1400 South Lake Shore Drive, Chicago, IL 60605, USA. E-mail: mwadhwa@fieldmuseum.org

experiments on the angrite analog composition (*18*) (Fig. 1A). This is expected because taking the ratio of distribution coefficients removes most of their compositional dependence.

Pyroxenes in the basaltic shergottites are particularly amenable to the application of a Eu oxybarometer because they show zonation in REE concentrations consistent with fractional crystallization from their parent magma (*21–23*). This implies that they have retained their original magmatic Eu/Gd ratios and remain unaltered by secondary processes. Additionally, high- and low-Ca pyroxenes (augites and pigeonites, respectively) are the first REE-bearing minerals to crystallize from the basaltic shergottite parent melt (*10*, *11*). Therefore, their Eu/Gd ratios are unaffected by prior crystallization of plagioclase (which scavenges Eu) and are predominantly a function of (i) magmatic redox conditions and (ii) the Eu/Gd ratio in the parent melt. Previous work has shown that the REE patterns of basaltic shergottite parent melts are parallel to those of their respective whole rocks (*13*, *21*, *23*, *24*). As a result, the Eu/Gd ratio in the parent melt of a basaltic shergottite is approximated by the Eu/Gd ratio in its whole rock, and thus D_{Eu}/D_{Gd} values for augites and pigeonites can be readily calculated. However, unlike for augite, there is no experimentally determined calibration curve of the relation between (D_{Eu}/D_{Gd}) and f_{O_2} for pigeonite. Therefore, of the two pyroxenes in the basaltic shergottites, only the augite is used to constrain f_{O_2} conditions.

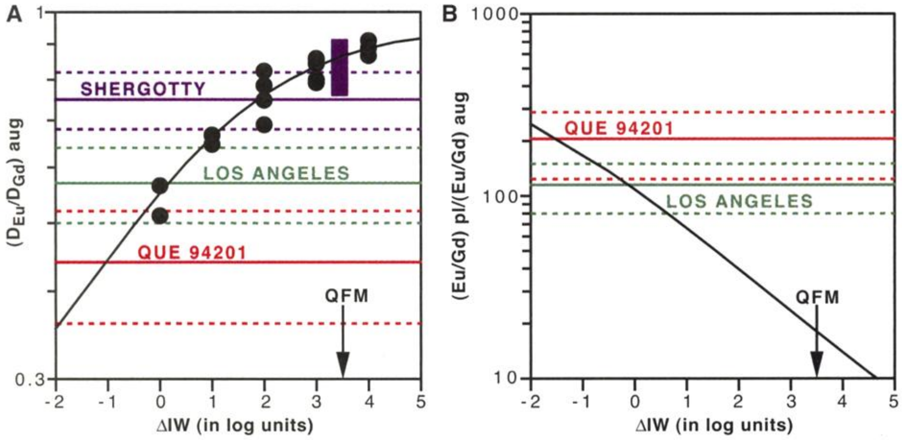

Fig. 1. (**A**) $(D_{Eu}/D_{Gd})_{augite}$ and (**B**) $(Eu/Gd)_{plagioclase}/(Eu/Gd)_{augite}$ versus f_{O_2} (in log units relative to the IW buffer) for the angrite basaltic system; solid black curves are theoretical best-fit curves to the experimental data of (*18*) [solid black circles in (A)]. Experimental data for shergottite augites (*19*, *20*) are shown as solid blue squares in (A). The $(D_{Eu}/D_{Gd})_{augite}$ value for Shergotty (solid blue line) and $(D_{Eu}/D_{Gd})_{augite}$ and $(Eu/Gd)_{plagioclase}/(Eu/Gd)_{augite}$ values for QUE 94201 (solid red lines) and Los Angeles (solid green lines) are also plotted; 2σ errors are shown as dashed lines.

The following basaltic shergottite samples were studied here: Shergotty, Zagami, lithologies A and B of EETA 79001 (*25*), Dar al Gani (DaG) 476, QUE 94201, and Los Angeles. Augite, which began crystallizing before plagioclase (*10*) in Shergotty, Zagami, EETA 79001, and DaG 476, records the oxidation state at the earliest stage in the crystallization history of these shergottites. However, in QUE 94201 and Los Angeles, differentiation processes resulted in the removal of the earliest augites (and pigeonites) from their parent melts before emplacement and crystallization. As a result, the crystallization record of these two shergottites begins with cosaturation of augite and plagioclase (*13*, *26*), and both these minerals reflect the magmatic redox state at this stage. Therefore, Eu and Gd concentrations were measured in augites in all of the basaltic shergottites and in plagioclase of QUE 94201 and Los Angeles, and D_{Eu}/D_{Gd} values for these minerals were calculated (*27*) (Table 1). Magmatic redox conditions for each of the basaltic shergottites were estimated by comparing their respective $(D_{Eu}/D_{Gd})_{augite}$ values with the curve in Fig. 1A. Additional constraints were obtained for the QUE 94201 and Los Angeles samples, using the relation between $(Eu/Gd)_{plagioclase}/(Eu/Gd)_{augite}$ and f_{O_2} shown in Fig. 1B. The f_{O_2} estimates obtained for QUE 94201 and Los Angeles using the augite data [from

Table 1. Eu and Gd abundances in parts per billion (ppb) and chondrite-normalized Eu/Gd ratios in augite of basaltic shergottites. Data are also given for plagioclase (shocked to feldspathic glass) in Los Angeles and QUE94201, in which augite and plagioclase may have cocrystallized. D_{Eu}/D_{Gd} values for augite and plagioclase are calculated by dividing Eu/Gd ratios in these minerals by Eu/Gd ratios in the respective whole rocks $[(Eu/Gd)_{WR}]$.

	Eu (ppb)*	Gd (ppb)*	Chondrite-normalized Eu/Gd*	Chondrite-normalized $(Eu/Gd)_{WR}$†	D_{Eu}/D_{Gd}	Estimated f_{O_2} (ΔIW)
Shergotty				0.87 ± 0.06		
Augite§	58 ± 3	315 ± 16	0.65 ± 0.05		0.75 ± 0.07	+1.9 (+0.9/−0.7)
Zagami				0.90 ± 0.06		
Augite§	103 ± 8	670 ± 59	0.54 ± 0.06		0.60 ± 0.08	+0.4 (+0.8/−0.7)
Los Angeles				0.92 ± 0.06		
Augite§	140 ± 11	946 ± 79	0.52 ± 0.06		0.57 ± 0.07	+0.2 (+0.6/−0.7)
Plagioclase§	270 ± 20	16 ± 4	60 ± 16		65 ± 20	−0.1 (+0.7/−0.8)‡
EETA 79001A				0.89 ± 0.09		
Augite§	56 ± 4	374 ±28	0.53 ± 0.06		0.59 ± 0.09	+0.3 (+0.9/−0.8)
EETA 79001B				0.87 ± 0.09		
Augite§	73 ± 5	630 ± 47	0.41 ± 0.04		0.47 ± 0.07	−0.7 (+0.6/−0.8)
DaG 476				0.71 ± 0.05		
Augite§	62 ± 5	607 ± 46	0.36 ± 0.04		0.50 ± 0.07	−0.5 (+0.7/−0.6)
QUE 94201				0.81 ± 0.12		
Augite§	56 ± 4	552 ± 28	0.36 ± 0.04		0.44 ± 0.08	−1.0 (+0.7/−0.9)
Plagioclase§	330 ± 25	16 ± 6	91 ± 38		91 ± 37	−1.5(+1.2/−1.0)‡

*Errors are 2σ from counting statistics only. †Whole-rock data for Shergotty, Zagami, Los Angeles, DaG 476, and QUE 94201 are from (*26*, *46*, *47*) and those for EETA 79001A and EETA 79001B are averages from whole-rock data sets compiled by (*48*); uncertainties are $\pm 2\sigma$. ‡Estimated from the relation between angritic $(Eu/Gd)_{plagioclase}/(Eu/Gd)_{augite}$ and f_{O_2}. §The major element composition of analyzed augites is as follows: Shergotty ($Wo_{33}En_{47}Fs_{20}$), Zagami ($Wo_{35}En_{44}Fs_{21}$), Los Angeles ($Wo_{33}En_{40}Fs_{27}$), EETA 79001A ($Wo_{26}En_{50}Fs_{24}$), EETA 79001B ($Wo_{31}En_{47}Fs_{22}$), DaG 476 ($Wo_{32}En_{50}Fs_{18}$), and QUE 94201 ($Wo_{38}En_{42}Fs_{20}$); that of analyzed plagioclase as follows: Los Angeles ($An_{56}Ab_{43}Or_1$) and QUE 94201 ($An_{63}Ab_{37}$).

$(D_{Eu}/D_{Gd})_{augite}$] and using the augite and plagioclase data [from $(Eu/Gd)_{plagioclase}/(Eu/Gd)_{augite}$ values] are consistent with each other (Table 1 and Fig. 1). This consistency provides further support for applying the f_{O_2} calibration curves obtained by (*18*) (shown as the solid black curves in Fig. 1, A and B) for the angrite system to the shergottite system.

The minimum and maximum $(D_{Eu}/D_{Gd})_{augite}$ values in Table 1 translate to redox estimates relative to the iron-wüstite (IW) buffer of –1.0 (+0.7/–0.9) and +1.9 (+0.9/–0.7), respectively. These values are systematically somewhat lower than those estimated from Fe-Ti oxides in shergottites (*11–14, 16*) which, for reasons noted earlier, may not record primary magmatic redox conditions. Nevertheless, the range of oxidation conditions recorded by the late-stage Fe-Ti oxide minerals (*14*) is, in fact, similar to that estimated here. Also, this variation in magmatic f_{O_2} of ~3 log units is likely to be robust because $(D_{Eu}/D_{Gd})_{augite}$ values estimated for each of the basaltic martian meteorites correlate with their initial Nd and Sr isotopic compositions (Fig. 2). Specifically, QUE 94201, which has the lowest $(D_{Eu}/D_{Gd})_{augite}$ value, also has the most positive initial ε(^{143}Nd) and lowest initial ^{87}Sr/^{86}Sr ratio; whereas Shergotty, with the highest $(D_{Eu}/D_{Gd})_{augite}$ value, has the most negative initial ε(^{143}Nd) and most radiogenic initial Sr isotopic ratio (and all other samples have intermediate values of these parameters) (Fig. 2). This suggests that the QUE 94201 parent melt, which represents a fractionated partial melt from a mantle source with a strong time-integrated light REE (LREE) depletion and was least affected by assimilation of a LREE-enriched component (*13, 28*), was also the most reduced of the basaltic shergottites. The redox state of a basaltic melt is inherited from its source and can subsequently be altered by processes such as assimilation, crystal fractionation, and volatile degassing. Figure 2 indicates that the oxidation condition of the basaltic shergottites is dominated by mixing of the redox signatures of a reduced source and an oxidized assimilant. Therefore, the f_{O_2} condition estimated for the parent melt of QUE 94201, which was only minimally (if at all) affected by assimilation, probably reflects the redox state of its source in the martian upper mantle.

The f_{O_2} estimate for the QUE 94201 parent melt can be further constrained from the range given in Table 1 of –1.9 to –0.3 (relative to the IW buffer) to a more plausible range of –1.0 to –0.3. This is because f_{O_2} conditions more than ~1 log unit lower than the IW buffer for a relatively FeO-rich parent magma (as is assumed for QUE 94201) would result in saturation of Fe metal (*29*). Therefore, the redox state of the QUE 94201 parent melt, and correspondingly of its source in the martian mantle, may be between ~IW –1.0 and ~IW –0.3 (that is, approaching that of the IW buffer). The higher f_{O_2} (by ~3 log units) inferred for the Shergotty parent melt is then most consistent with assimilation of an even more oxidized component, which is also responsible for the negative initial ε(^{143}Nd) value and radiogenic initial Sr composition of this basaltic shergottite. The crust of Mars is the most obvious candidate to fulfill the isotopic and geochemical requirements for such a component (*30*). Therefore, the trends in Fig. 2 indicate that parent melts of all the basaltic shergottites originated from an upper mantle source on Mars having a redox state close (within ~1 log unit) to that of the IW buffer. Subsequently, these parent melts interacted to different degrees with an oxidized component [with a redox state possibly higher than or equal to that of the quartz-fayalite-magnetite (QFM) buffer], the isotopic characteristics of which are most consistent with it being the martian crust. QUE 94201 is least affected by the assimilation of this oxidized crustal component, Shergotty seems most affected, and the other basaltic shergottites are affected to intermediate degrees.

The reason for the occurrence on Mars of two reservoirs distinct in their oxidation state (a reduced mantle source at ~IW and an oxidized crust at ≥ ~QFM) is unclear. However, an explanation may lie in the systematic variations seen in the redox conditions of terrestrial igneous rocks. On Earth, the oxidation state of a particular suite of rocks correlates strongly with the tectonic environment (*31–33*). In particular, redox conditions for all but subduction-related magmas lie between wüstite-magnetite and QFM, whereas magmas crystallizing in the more hydrated subduction terrains are more oxidized and lie between nickel-nickel oxide and magnetite-hematite. Furthermore, although the redox state of the Earth's "uncontaminated" mantle (unaltered by crustal recycling and hydrous alteration) is uncertain, it may be as reduced as several log units below QFM (*34*).

By analogy, it can be inferred that the reduced conditions (close to ~IW) estimated in the mantle source of the basaltic shergottites may reflect the primary redox state of Mars' upper mantle. Moreover, the crustlike component assimilated to varying degrees by these basalts is oxidized relative to this mantle source (by >3 log units), possibly through a process such as hydration and aqueous alteration. This is supported by recent work that shows that the parent magma of Shergotty, the most oxidized of the basaltic shergottites studied here, may have contained as much as ~1.8 weight % water (*35*). Other recent studies suggesting that the crust of Mars is more hydrated than previously estimated (*36, 37*) also support water as the main crustal oxidant. A corollary drawn from these arguments is that, in contrast to Earth, Mars did not have any substantial recycling of this oxidized crust and that its reduced upper mantle has, therefore, remained uncontaminated by this crustal reservoir.

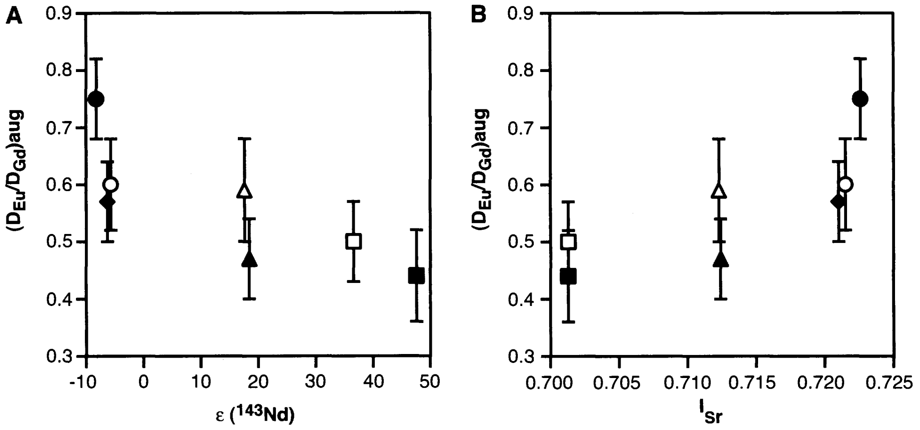

Fig. 2. $(D_{Eu}/D_{Gd})_{augite}$ versus (**A**) initial ε (^{143}Nd) (*39*) and (**B**) initial ^{87}Sr/^{86}Sr ratios for Shergotty (●), Zagami (○), Los Angeles (◆), EETA 79001A (△), EETA 79001B (▲), DaG 476 (□), and QUE 94201 (■). Errors are ±2σ. Nd and Sr isotopic data are from (*28, 40–44*). Nd isotopic data for Los Angeles are from (*44*). The initial Nd and Sr isotopic composition for Shergotty, Zagami, EETA 79001A, and EETA 79001B are calculated from their whole rock data, assuming a crystallization age of 180 million years ago. Initial Nd and Sr data for QUE 94201, DaG 476, and Los Angeles are actual measured values [except for the initial Sr isotopic value for DaG 476, which is a best estimate (*44*)]. Extrapolation of these data to 180 million years ago would only change the initial Nd and Sr isotopic composition marginally and would not affect the trends shown in these figures.

References and Notes

1. J. F. Bell III, in *Mineral Spectroscopy: A Tribute to Roger G. Burns*, M. D. Dyar, C. McCammon, M. W. Schaefer, Eds. (*Geochem. Soc. Spec. Publ. 5*, Lancaster Press, Lancaster, PA, 1996), pp. 359–380.
2. D. L. Anderson, *J. Geophys. Res.* **77**, 789 (1972).
3. T. R. McGretchin, J. R. Smyth, *Icarus* **34**, 512 (1978).
4. J. W. Morgan, E. Anders, *Geochim. Cosmochim. Acta* **43**, 1601 (1979).

5. *Basaltic Volcanism on the Terrestrial Planets*, R. B. Merrill, R. Ridings, Eds. (Pergamon, New York, 1981), pp. 633–699.
6. K. A. Goettel, *Carnegie Inst. Wash. Yearb.* **82**, 363 (1983).
7. G. Dreibus, H. Wänke, *Meteoritics* **20**, 367 (1985).
8. ———, *Icarus* **71**, 225 (1987).
9. J. Longhi, E. Knittle, J. R. Holloway, H. Wänke, in *Mars*, H. H. Kieffer, B. M. Jakovsky, C. W. Snyder, M. S. Matthews, Eds. (Univ. of Arizona Press, Tucson, AZ, 1992), pp. 184–208.
10. H. Y. McSween Jr., *Meteoritics* **29**, 757 (1994) and references therein.
11. E. M. Stolper, H. Y. McSween Jr., *Geochim. Cosmochim. Acta* **43**, 1475 (1979).
12. J. V. Smith, R. L. Hervig, *Meteoritics* **14**, 121 (1979).
13. H. Y. McSween Jr., D. D. Eisenhour, L. A. Taylor, M. Wadhwa, G. Crozaz, *Geochim. Cosmochim. Acta* **60**, 4563 (1996).
14. C. D. K. Herd, J. J. Papike, *Meteorit. Planet. Sci.* **35** (suppl.), A70 (2000).
15. S. Ghosal, R. O. Sack, M. S. Ghiorso, M. Lipschutz, *Contrib. Mineral. Petrol.* **119**, 197 (1998).
16. V. P. S. Hale, H. Y. McSween Jr., G. A. McKay, *Geochim. Cosmochim. Acta* **63**, 1459 (1999).
17. G. A. McKay, in *Geochemistry and Mineralogy of Rare Earth Elements*, B. R. Lipin, G. A. McKay, Eds., *Reviews of Mineralogy 21* (Mineralogical Society of America, Washington DC, 1989), pp. 45–77 and references therein.
18. G. A. McKay, L. Le, J. Wagstaff, G. Crozaz, *Geochim. Cosmochim. Acta* **58**, 2911 (1994).
19. G. A. McKay, J. Wagstaff, S.-R. Yang, *Geochim. Cosmochim. Acta* **50**, 927 (1989).
20. G. McKay, personal communication.
21. M. Wadhwa, H. Y. McSween Jr., G. Crozaz, *Geochim. Cosmochim. Acta* **58**, 4213 (1994).
22. M. Wadhwa, G. Crozaz, L. A. Taylor, H. Y. McSween Jr., *Meteorit. Planet. Sci.* **33**, 321 (1998).
23. M. Wadhwa, R. C. F. Lentz, H. Y. McSween Jr., G. Crozaz, *Meteorit. Planet. Sci.* **36**, 195 (2001).
24. L. L. Lundberg, G. Crozaz, G. McKay, E. Zinner, *Geochim. Cosmochim. Acta* **52**, 2147 (1988).
25. EETA 79001 is the only known meteorite with two lithologies in igneous contact (*38*).
26. A. E. Rubin *et al.*, *Geology* **28**, 1011 (2000).
27. The following thin sections were studied: Shergotty (USNM 321-6), Zagami (USNM 6473-2), EETA 79001A (.317), EETA 79001B (.318), DaG 476 (MPI PTS 3), QUE 94201 (.5), and Los Angeles (UCLA PTS 748); numbers in parentheses are thin-section identification numbers. Sections of Shergotty and Zagami were documented with the University of Chicago JEOL JEM-5800LV scanning electron microscope and the Cameca SX-50 electron microprobe; the Los Angeles section was characterized with the University of Chicago and University of Tennessee Cameca SX-50 electron microprobes. Documentation of EETA 79001 lithologies A and B, QUE 94201, and DaG 476 sections was available from our previous studies (*21–23*). In each section, augite with the lowest Fe/Mg ratio (that is, the earliest to begin crystallization) was selected for analysis with the ion microprobe. Additionally, in the QUE 94201 and Los Angeles samples, feldspathic glass areas having the highest Ca contents (representing the earliest formed plagioclase grains) were also selected for analysis. Eu and Gd abundances were measured in situ with the Washington University modified Cameca IMS-3f ion microprobe; primary beam currents as well as counting times on the appropriate masses were increased by a factor of 2 to 3 as compared to those in our previous studies of martian meteorites (*21–23*). 2σ errors (from counting statistics) on Eu and Gd concentrations were ~5 to 8%.
28. L. E. Borg, L. E. Nyquist, L. A. Taylor, H. Weismann, C.-Y. Shih, *Geochim. Cosmochim. Acta* **61**, 4915 (1997).
29. E. M. Stolper, *Geochim. Cosmochim. Acta* **41**, 587 (1977).
30. J. H. Jones, *Geochim. Cosmochim. Acta* **50**, 969 (1989).
31. B. J. Wood, L. T. Bryndzia, K. E. Johnson, *Science* **248**, 337 (1990).
32. S. E. Haggerty, L. A. Tompkins, *Nature* **303**, 295 (1983).
33. D. M. Christie, I. S. E. Carmichael, C. H. Langmuir, *Earth Planet Sci. Lett.* **79**, 397 (1986).
34. S. K. Saxena, *Geochim. Cosmochim. Acta* **53**, 89 (1989).
35. H. Y. McSween *et al.*, *Nature* **409**, 487 (2001).
36. M. C. Malin, K. S. Edgett, *Science* **288**, 2330 (2000).
37. L. L. Leshin, *Geophys. Res. Lett.* **27**, 2017 (2000).
38. H. Y. McSween, E. Jarosewich, *Geochim. Cosmochim. Acta* **47**, 1501 (1979).
39. Initial ε (^{143}Nd) is defined as the initial ^{143}Nd/^{144}Nd ratio of the sample relative to the ^{143}Nd/^{144}Nd ratio in the chondritic uniform reservoir (CHUR), in parts per 10^4.
40. L. E. Nyquist *et al.*, *Geochim. Cosmochim. Acta* **43**, 1057 (1979).
41. L. E. Nyquist, B. Bansal, H. Weismann, C.-Y. Shih, *Lunar Planet. Sci.* **XXVI**, 1065 (1995).
42. C.-Y. Shih *et al.*, *Geochim. Cosmochim. Acta* **46**, 2323 (1982).
43. J. L. Wooden *et al.*, *Lunar Planet. Sci.* **XIII**, 879 (1982).
44. L. E. Borg, L. E. Nyquist, H. Wiesmann, Y. Reese, J. J. Papike, *Lunar Planet. Sci.* **XXXI** (abstr. 1036) (2000) [CD-ROM].
45. L. E. Nyquist, Y. Reese, H. Wiesmann, C.-Y. Shih, *Lunar Planet. Sci.* **XXXII** (abstr. 1407) (2001) [CD-ROM].
46. J. A. Barrat, J. Blichert-Toft, R. W. Nesbitt, F. Keller, *Meteorit. Planet. Sci.* **36**, 23 (2001).
47. G. Dreibus *et al.*, *Meteorit. Planet. Sci.* **31** (suppl.), A39 (1996).
48. C. Meyer, *NASA Johnson Space Center Publication 27672*, Revision A, 88 (1998).
49. Thin sections were provided by the Max-Planck-Institut für Chemie (Mainz), the Meteorite Working Group, the National Museum of Natural History (Washington, DC), and the University of California at Los Angeles. I thank I. Steele and N. Heim for help with documentation of sections at the University of Chicago; H. McSween and R. Lentz for additional documentation for the DaG 476, QUE 94201, and Los Angeles sections; G. McKay for making his REE partitioning data readily available; G. Crozaz for access to the Washington University ion microprobe; and L. Borg, G. Crozaz, J. Jones, G. Lugmair, H. McSween, and two anonymous reviewers for their insightful comments and discussions, which helped to improve this manuscript. Supported by NASA and NSF.

20 November 2000; accepted 16 January 2001

Impact Event at the Permian-Triassic Boundary: Evidence from Extraterrestrial Noble Gases in Fullerenes

Luann Becker,[1]* Robert J. Poreda,[2] Andrew G. Hunt,[2] Theodore E. Bunch,[3] Michael Rampino[4]

The Permian-Triassic boundary (PTB) event, which occurred about 251.4 million years ago, is marked by the most severe mass extinction in the geologic record. Recent studies of some PTB sites indicate that the extinctions occurred very abruptly, consistent with a catastrophic, possibly extraterrestrial, cause. Fullerenes (C_{60} to C_{200}) from sediments at the PTB contain trapped helium and argon with isotope ratios similar to the planetary component of carbonaceous chondrites. These data imply that an impact event (asteroidal or cometary) accompanied the extinction, as was the case for the Cretaceous-Tertiary extinction event about 65 million years ago.

The extinction event that marks the Permian-Triassic boundary (PTB) [251.4 ± 0.3 million years ago (Ma)] was the most severe in the past 540 million years (*1*), killing off over 90% of all marine species, ~70% of terrestrial vertebrate genera, and most land plants (*2–5*). Several new studies have shown that these extinctions were much more abrupt than previously thought (*6–8*), with estimates of the extinction interval ranging from <500,000 years (*6*) to ~8000 years (*8*). Proposed catastrophic hypotheses for the PTB extinction event include bolide impact (asteroidal or cometary) (*9*) and/or massive flood basalt volcanism (*10*). The radiometric ages of the Siberian Flood Basalt volcanism (251.2 ± 0.3 Ma) (*6*, *10*) suggest that the volcanism was coincident with the time of the PTB extinction event. Other extinction mechanisms involving ocean anoxia as well as changes in sea level and climate have also been proposed (*1*, *11*, *12*).

The suggestion by Alvarez *et al.* (*13*, *14*) that bolide impact was the ultimate reason for the mass extinction observed at the 65–million year Cretaceous-Tertiary boundary (KTB) led to the assumption that all such events were associated with an extraterrestrial (ET) cause. Despite a compelling ET scenario developed for the KTB (supported by the presence of iridium, shocked quartz, and microspherules), the cause of the PTB mass extinction remains unresolved. One of

---

[1] Department of Earth and Space Sciences, University of Washington, Box 351310, Seattle, WA 98195–1310 USA. [2] Department of Earth and Environmental Sciences, University of Rochester, Rochester, NY 14627, USA. [3] Space Science Division, Ames Research Center, National Aeronautics and Space Administration, Moffett Field, CA 94035, USA. [4] New York University, New York, NY 10003, USA, and NASA, Goddard Institute of Space Studies, New York, NY 10025, USA.

*To whom correspondence should be addressed. E-mail: lbeck00@u.washington.edu or lbecker@soest.hawaii.edu